Chapter 3

Effects of Short-Chain Alcohols and Pyridine on the Hydration Forces between Silica Surfaces

3.1 Introduction

The DLVO theory (1,2) states that the total interaction force (F_t) between two lyophobic particles in a medium can be expressed as a sum of the electrical double-layer force (F_e) and the van der Waals force (F_d) as follows:

$$F_t = F_e + F_d \qquad [1]$$

However, direct measurement of surface forces conducted in aqueous media showed the existence of forces not considered in the DLVO theory. These include the hydrophobic and hydration forces. The former was observed with mica and silica surfaces coated with surfactants (3,4,5), while the latter was observed with silica surfaces (6-10) and lecithin bilayers (11). Derjaguin and Churaev (12) suggested, therefore, that the DLVO theory is applicable only to those colloidal particles whose water contact angles (θ) are in the range 15^o-64^o. When θ is outside this range, the DLVO theory may be extended to include the contributions from the extraneous forces, as follows:

$$F_t = F_e + F_d + F_S \qquad [2]$$

where F_s represents the hydrophobic or hydration force, which are collectively referred to as structural force.

Rabinovich, *et al.*(6) measured the surface forces between glass fibers in KCl solutions to

show the existence of hydration force with a decay length of 0.85 nm. The results showed also that the hydration force decreases with increasing electrolyte concentration. Similar results were obtained by Peschel, *et al.*(7), who conducted force measurements between polished silica plates in different electrolyte solutions. They showed that decay length decreases with increasing electrolyte concentration, and that the decrease becomes more significant in the order of KCl<NaCl<LiCl. The authors suggested that the difference in the chemical potentials of the Li^+ ions at the surface and in the bulk of water is small, as compared to those for Na^+ and K^+ ions, because the Li^+ ions are more potent structure-forming ions. The small difference in chemical potentials results in a low disjoining pressure. Horn, *et al.*(8) conducted direct force measurements using the surface force apparatus (SFA) with flamed silica with an advancing water contact angle of 45^o. Despite the considerable hydrophobicity, the silica surface exhibited hydration forces at distances less than 3 nm. Later work by Grabbe and Horn (9) showed that hydration force changes little with the changes in surface treatment and electrolyte concentration. The measured hydration forces could be fitted to a double-exponential function of the form:

$$\frac{F_{hyd}}{R} = C_1 \exp\left(-\frac{H}{D_1}\right) + C_2 \exp\left(-\frac{H}{D_2}\right) \qquad [3]$$

with C_1=140 mJ/m^2, C_2=5.4 mJ/m^2, D_1=0.057 nm and D_2=0.57 nm. Ducker *et al.*(10) used an atomic force microscope (AFM) to measure the surface forces between silica sphere and silica plate in NaCl solutions, and observed hydration forces at H<15 nm.

The existence of hydration forces may be useful for explaining the difficulty in predicting the stability of silica suspensions using the DLVO theory. It has been shown that very high concentrations of electrolyte are needed to destabilize Ludox silica suspensions particularly at low pHs where the particles exhibit low ς-potentials (13). Watillon and Gerard (14) ascribed the exceptional stability of silica suspensions to the 'steric barrier' created by the immobilized monolayer of water molecules on the surface.

Unlike silica, direct force measurements conducted with mica surfaces exhibit no hydration

forces in pure water. At electrolyte concentrations higher than approximately 10^{-3} M, however, mica surfaces showed extra repulsion at short separation distances (15,16). This is believed to originate from the excess work required to displace the water molecules from the hydrated cations that are adsorbed on mica surfaces. Since the extra repulsion is caused by adsorbed cations, rather than the inherent property of mica, it is referred to as 'secondary hydration' force. The hydration force observed with silica, on the other hand, is caused by the inherent property of the solid; therefore, it is referred to as 'primary hydration' force (17). The force data obtained with mica surfaces in 1:1 electrolyte solutions can be fitted to Eq. [3] with D_1in the range 0.17-0.3 nm and D_2 in the range 0.6-1.2 nm. In general, D_2 increases with increasing hydration energy of the cations. Thus, the decay length decreases in the order of $Li^+ > Na^+ > K^+ > Cs^+$, which is the opposite of the series exhibited with the primary hydration force.

It is interesting that the secondary hydration forces observed with mica are oscillatory with a periodicity of roughly the diameter of water molecules (16,18). The authors suggested, therefore, that the hydration forces are due to ordered layering of the water molecules on the surface. However, the hydration forces observed with silica are monotonic, indicating that there are possibly no ordered layers of water molecules on silica. It is possible, on the other hand, that the oscillation may smear out on silica surface due to its roughness, even if there exists a well-defined water structure in the vicinity of silica surface (19). Nevertheless, the lack of oscillations plus the fact that the measured hydration forces are time-dependent led Vigil, *et al*. (20) to believe that the primary hydration forces are due to the steric repulsion between the silicic acid hair formed on the surface. That the hydration force decreases in electrolyte solutions has been attributed to the collapse of the silicic acid hair due to charge neutralization or double-layer compression. More recently, Yaminsky, *et al* (21) showed that the surface forces measured with silica vary widely depending on the methods of preparing the surface.

With an aim to further study the origin of the primary hydration force, we conducted direct force measurements between fully hydroxalated silica plate and glass sphere in aqueous solutions containing various organic solutes. The measurements were made using a Digital Instruments Nanoscope III atomic force microscope. It was shown earlier by one of us that the stability of

silica suspensions decreases with increasing ethanol concentration (22). This observation was made at pH 2 (p.z.c. of silica), where there are no double-layer forces at play. It was concluded, therefore, that destabilization of silica suspensions by ethanol is due to the decrease in the repulsive hydration force. In the present communication, we report the results of the surface force measurements conducted between silica surfaces in solutions containing ethanol, methanol, trifluoroethanol (TFE) and pyridine. The solutes used here have different basicities (pK_b); therefore, they should react differently with the silanol (Si-OH) groups on the surface of silica. It would be of interest to see how this affects the surface forces between silica surfaces, particularly the hydration force component at short range.

3.2 Experimental

3.2a *Sample Preparation*

Optically smooth fused silica plates were obtained from Haraeus Amersil, Inc. They were cleaned by boiling in a nitric acid solution for about 12-15 hours, and then equilibrated in conductivity water from a Barnstead Nanopure II water treatment unit. Clean silica plates thus obtained exhibited an equilibrium contact angle (θ_{eq})<5°, as measured using a Ramé-Hart Model 100 goniometer. Glass spheres of radius 10-30 μm from Duke Scientific were mounted on cantilever tips by means of an adhesive (Epon R Resin 1004, Shell Chemical Company) (10,23), placed in NaOH solutions (pH~10.0) overnight, and equilibrated in Nanopure water before each experiment. HPLC-grade methanol, pyridine and TFE were obtained from Aldrich Chemical Co., while absolute 200-proof (ACS grade) ethanol was obtained from Aaper Alcohol and Chemical Company.

3.2b *Methods and Apparatus*

A Digital Instruments Nanoscope III AFM was used to measure the forces between a silica plate and a glass sphere mounted at the tip of a cantilever. Standard triangular silicon nitride

cantilevers were obtained from Digital Instruments Co. The stiffness of the cantilevers was measured by the technique of Senden and Ducker (24). This consists of placing a heavy tungsten sphere on the cantilever tip, turning the cantilever upside down and measuring its deflection from the AFM signal. The glass spheres were mounted on the cantilever tip by means of a micromanipulator. The mounted spheres, equilibrated in NaOH solutions and Nanopure water as explained in the last section, were then transferred to a fluid cell for force measurements. Force measurements were conducted in Nanopure water and in solutions containing aliquots of ethanol, methanol, trifluoroethanol and pyridine. The radius of the glass spheres was measured using a Kontron SEM-IPS image processing system.

3.3 Results

Figure 3.1 shows the results of the force measurements conducted with silica plate and glass sphere in Nanopure water and in solutions of 10 and 20% by volume ethanol. The dotted lines represent DLVO fits of the experimental data obtained using an algorithm developed by Chan, *et al* (25). Table 3.1 gives the values of the Hamaker constant (A_{131}), where the subscripts **1** and **3** represent silica and solution phases, respectively, and the surface potentials ($\psi_{0(\infty)}$) at infinite separation distances that were used to fit the data. Since the amounts of alcohol used in the force measurements were high, it was necessary to calculate the values of A_{131} using the following expression (19):

$$A_{131} = \frac{3}{4}kT\left(\frac{\varepsilon_1 - \varepsilon_3}{\varepsilon_1 + \varepsilon_3}\right)^2 + \frac{3h\nu_e}{16\sqrt{2}}\frac{\left(n_1^2 - n_3^2\right)^2}{\left(n_1^2 + n_3^2\right)^{3/2}} \qquad [4]$$

where k is the Boltzmann constant, T the absolute temperature, ε_1 (=3.8) the dielectric constant of silica, ε_3 the same of the medium (see Table 3.1), h the Planck's constant, ν_e the UV absorption frequency, n_1 (=1.448) the refractive index of silica, n_3 the same of the medium. The values of ε_3 and n_3 for the media used in the force measurements conducted in the present work are given in

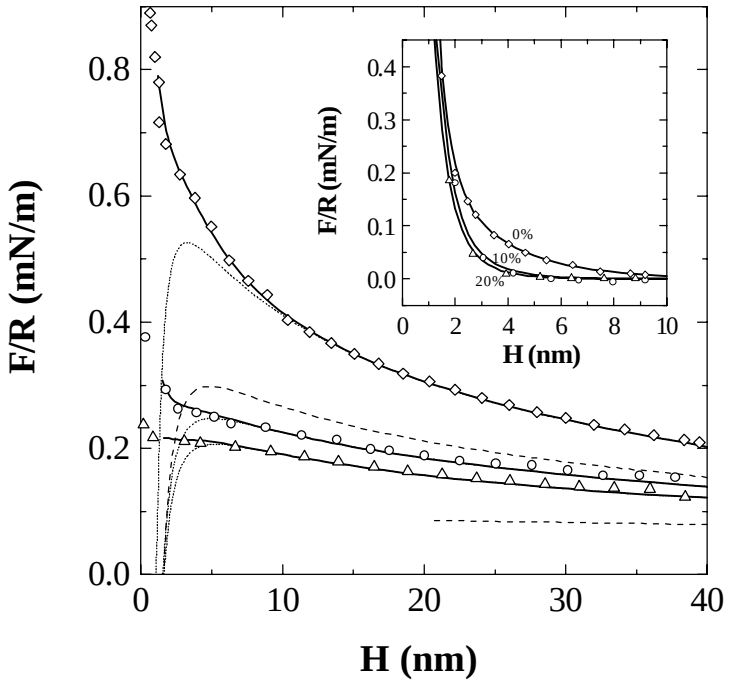

Figure 3.1. *F/R* vs. *H* curves obtained in Nanopure water (◊), 10% ethanol (○), and 20% ethanol (Δ) solutions. The dotted lines represent the DLVO theory fitted to the experimental data in Nanopure water (constant charge model) and in ethanol solutions (charge regulation model). The dashed lines represent the constant charge (upper curve) and constant potential (lower curve) models of the DLVO theory fitted to the data obtained in the 10% ethanol solution. The solid lines represent the extended DLVO fits (Eq. [2]) incorporating a hydration force term. The inset shows the hydration force curves (Eq. [3]) alone.

Table 3.1

The Values of ε_3 and n_3 Used to Calculate A_{131} Using Eq. [4] and the Double-Layer Constants Obtained From the Force Curves

Solutes	ε_3	n_3	A_{131} (10^{-21} J)	ψ_0 (mV)	κ^{-1} (nm)
TFE (10%)	-	-	5.86[4]	64.0	103
Ethanol (10%)	74[1]	1.3379[3]	5.86[4]	60.0	176
(20%)	69.5[1]	1.3438[3]	5.47[4]	59.3	196
Water	80[2]	1.333[3]	6.30[4]	58.0	96
Methanol (15%)	73.4[1]	1.3358[3]	3.0[4]	61.7	202
Pyridine (2%)	-	-	6.30[4]	58.0	55

[1]Ref (26); [2,3]CRC handbook; [4]from Eq. [4]

Table 3.1. The values of ε_3 for the 10 and 20% ethanol solutions and for the 15% methanol solution were obtained by interpolating the values reported by Kosmulski and Matijevic (26). These values were also used for calculating the double-layer forces using the algorithm of Chan, *et al* (25). The values of ν_e for water and ethanol have been reported to be 3.0×10^{15} s^{-1}, while the same for fused silica[25] is 3.2×10^{15} s^{-1}. The value of ν_e for methanol is not known; however a Cauchy plot (27) showed that its value is practically the same as those for water and ethanol. In using Eq. [4], ν_e was substituted by the arithmetic mean (3.1×10^{15} s^{-1}) of the values for silica and the medium, as suggested in ref 25.

At large separation distances (H), the results obtained in Nanopure water can be fitted to the constant charge model with $\psi_{0(\infty)}$=-58 mV, κ^{-1} (Debye length) =96 nm, and $A_{131}=6.3 \times 10^{-21}$ J. On the other hand, the data obtained in ethanol solutions fit the charge regulation model with $\psi_{0(\infty)}$=-60 mV, κ^{-1}=176 nm at 10% ethanol; and $\psi_{0(\infty)}$=-59.3 mV with κ^{-1}=196 nm at 20% ethanol. As shown, the forces measured at distances below approximately 10 nm are larger than predicted by the DLVO theory. The extraneous repulsion at short distances may be due to the hydration force, which apparently decreases with increasing ethanol content in water.

In order to estimate the changes in magnitude of the hydration force, the force data were fitted to the extended DLVO theory (Eq. [2]), as shown by the solid lines in Figure 3.1. Eq. [2] includes the double-exponential force law (Eq. [3]) to represent the hydration force. The hydration force measured in Nanopure water can be fitted to Eq. [3] with the following parameters: C_1=8.0 mN/m, D_1=0.4 nm, C_2=0.35 mN/m, D_2=2.4 nm. These values are close to those estimated by Yotsumoto and Yoon (17) based on the data obtained from turbidity measurements. The hydration forces measured in ethanol solutions have been fitted with the parameters given in Table 3.2. Note that D_2 decreases from 2.4 nm in Nanopure water to 1.2 and 1.1 nm in 10 and 20% ethanol solutions, respectively. The inset of Figure 3.1 shows the changes in the hydration forces with separation distance (H) in Nanopure water and in 10 and 20% ethanol solutions. The data points given in the inset have been obtained by subtracting the contributions from the electrostatic and dispersion forces, while the solid lines represent Eq. [3]. Thus, the hydration force decreases substantially in 10% ethanol solution. Apparently, further increase in

Table 3.2

Comparison of the pK_b Values of the Solutes and the Hydration Force Constants of Eq. [3]

Solutes	pK_b	C_1 (mN/m)	D_1 (nm)	C_2 (mN/m)	D_2 (nm)
TFE	-	6.5	0.43	0.33	2.10
Ethanol (10%)	17.1	5.0	0.48	0.42	1.25
(20%)	17.1	3.27	0.50	0.43	1.10
Water	15.7	7.2	0.44	0.35	2.40
Methanol	15.2	-	-	-	-
Pyridine	8.75	8.0	0.41	0.35	2.30

ethanol concentration does not reduce the hydration force significantly.

Figure 3.2 compares the force curves obtained in a 15% methanol solution and in Nanopure water. The former can be fitted to the DLVO theory with $\psi_{0(\infty)}$=-61.7 mV, κ^{-1}=124 nm, and A_{131}=3.0x10^{-21} J. The two silica surfaces jump into contact at H≈2.8 nm, most likely due to the attractive van der Waals force. When the two surfaces are separated from each other, a small pull-off force (0.07-0.1 mN/m), which is also known as the adhesion force was observed. It should be noted here that both in Nanopure water and in ethanol solutions, the adhesion forces were zero. The force curve obtained in the methanol solution has been re-plotted in the inset at a larger scale to more clearly show the jump distance. The fact that the two surfaces jump into contact provides strong evidence that the hydration force observed in Nanopure water disappears completely in the presence of 15% methanol. As with ethanol, the charge regulation model fits the data better than the constant charge or constant potential model.

It should be noted here that the value of A_{131}=3.0x10^{-21} J that was used to fit the force curve obtained in the 15% methanol solution is lower than that (6.0x10^{-21} J) calculated using Eq. [4]. There may be two possible causes for this discrepancy. *First*, the jump distance measured in the present work may include a small error, as it should vary with the stiffness of the cantilever spring. Furthermore, there are uncertainties in determining the zero-separation distance with AFM, which should also affect the jump distance. *Second*, A_{131} may decrease in methanol solutions. It is likely that the methanol concentration increases with decreasing surface separation. There are thermodynamic reasons that methanol displaces water from the surface of silica, as will be discussed later in this communication. The fact that the force data fit the charge regulation model may also support this view. If the medium was 100% methanol, Eq. [4] gives a value A_{131}=3.7x10^{-21} J, which is closer to the value obtained from the force measurement.

Figure 3.3 shows the results of the force measurements conducted between glass sphere and silica plate in 10% TFE and 2% pyridine solutions. TFE was chosen because it is less basic than ethanol due to fluorine substitution of hydrogen, and pyridine was chosen because it is more basic than ethanol and methanol. Attempts were made to fit the data to the DLVO theory. However,

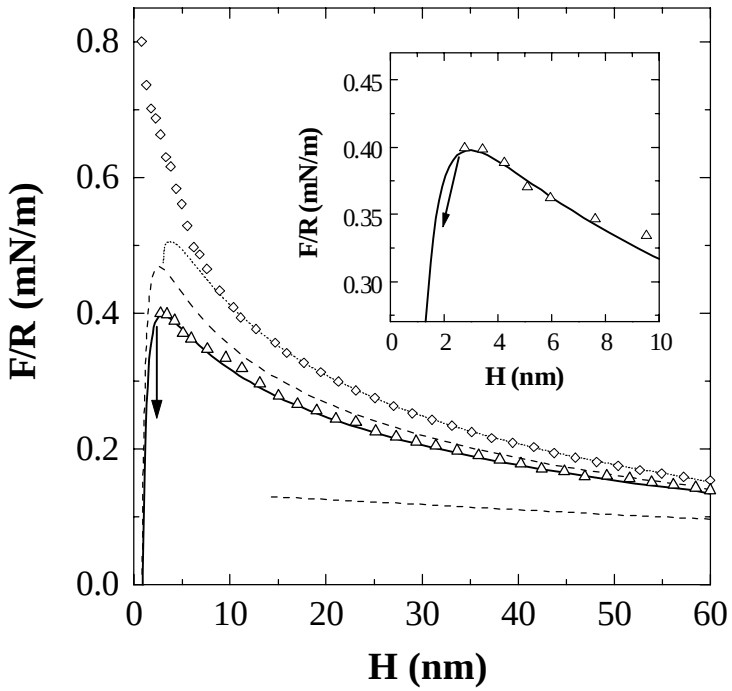

Figure 3.2. *F/R* vs. *H* curves obtained in Nanopure water (◊) and in 15% methanol (Δ) solutions. The dotted line represents the constant charge model of the DLVO theory fitted to the data obtained in Nanopure water. The solid line represents the charge regulation model of the DLVO theory fitted to the data obtained in the methanol solution. The dashed lines represent the constant charge (upper curve) and constant potential (lower curve) models of the DLVO theory fitted to the data obtained in 15% methanol solution. The inset shows the data obtained in methanol solution on a magnified scale. The jump occurs at the distance predicted by the DLVO theory, indicating that the hydration force disappears in 15% methanol solution.

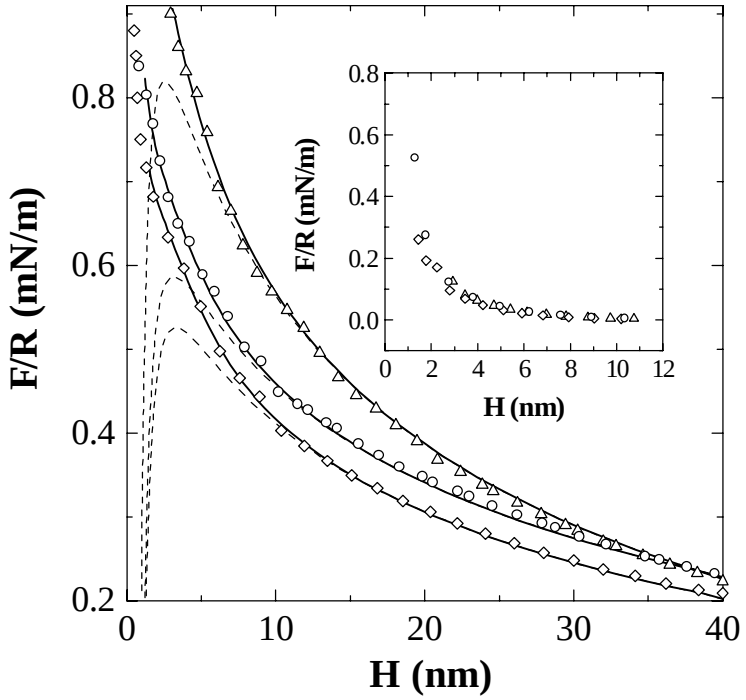

Figure 3.3. F/R vs. H curves obtained in Nanopure water (◊), 10% trifluoroethanol (O) and 2% pyridine (Δ) solutions. The dotted lines represent the constant charge model of the DLVO theory fitted to the experimental data points obtained at large surface separations. The solid line represents the same data fitted to the extended DLVO theory with a hydration force term (Eq. [2]). The inset shows the hydration forces alone.

only the data obtained at large separations can be fitted to the theory, as is the case with the force curve obtained in Nanopure water, which is also shown in Figure 3.3 for comparison. The data obtained in both the TFE and pyridine solutions were fitted to the constant charge model with the parameters given in Table 3.1. The value of A_{131} that was used to fit the data obtained in 10% TFE solution was assumed to be the same as that in 10% ethanol solution due to the lack of appropriate information. On the other hand, the data obtained in the 2% pyridine solution were fitted to the DLVO theory with the value of A_{131} that is the same as that of water.

The force data obtained at short separations have been fitted to the extended DLVO theory, shown by the solid lines in Figure 3.3, with the hydration force parameters given in Table 3.2. Note that D_2 values obtained in TFE and pyridine solutions are close to that obtained in Nanopure water. The hydration force does not change significantly in these solutions, as shown by the force curves given in the inset of Figure 3.3. Also, similar to the results obtained in Nanopure water and ethanol solutions, no adhesion forces were observed between silica surfaces when they were separated from contact in both TFE and pyridine solutions.

3.4 Discussions

The values of $\psi_{0(\infty)}$ for silica, listed in Table 3.1, suggest that the surface potential does not change significantly in solutions containing varying quantities of alcohol, TFE, and pyridine. This is consistent with the observations of Kosmulski and Matijevic (26) that the ς-potentials of silica do not change significantly with solvents of varying compositions of alcohols (up to 20% by weight in the pH range of 5-7). On the other hand, κ^{-1} varies from 55 nm at 2% pyridine to 202 nm at 15% methanol. The lower dielectric constant of ethanol and methanol solutions, as compared to that of water, should decrease κ^{-1}; hence, the changes in the Debye length cannot be accounted for by the changes in ε. Therefore, the changes in κ^{-1} should be attributed to the changes in back ground electrolyte concentration. The pH measured in the 2% pyridine solution was about 9.4. The Debye length calculated at H^+ ion concentration of $10^{-9.3}$ M is 59.8 nm, which is in reasonable agreement with the value of 55 nm obtained by fitting the force data to the DLVO

theory. The Debye lengths obtained from the force curves obtained in ethanol and methanol solutions suggest a 67-80% decrease in the background electrolyte concentration from that of Nanopure water. It is difficult, however, to measure the pH of solutions containing 10-20% by volume alcohol to determine the changes in H^+ ion concentration. Note that the value of κ^{-1} obtained for the 10% TFE solution is smaller than those for solutions containing methanol and ethanol, which may be attributed to the fact that the former is more acidic than the latter.

Table 3.2 lists the values of the basicity (pK_b) of all the solutes used in the present communication. The pK_b values for methanol and ethanol were calculated from the known pK_a values (28), the autoprotolysis constant (pK_{auto}) (29), and the pK_w for water. TFE is known to be a weaker base than ethanol because of the three electronegative fluorine atoms; however, its pK_b is not known. The pK_b value for pyridine was calculated from its pK_a value (28) and the pK_w for water. Pyridine is basic because of the lone pair of electrons on the nitrogen atom. The basicity increases upon going down the table, i.e., TFE is probably the least basic and pyridine is the most.

Table 3.2 also includes the hydration force parameters C_1, D_1, C_2, and D_2 obtained from the force measurements conducted in the present work. It may be difficult to deduce a meaningful relationship between the values of C_1 and the interfacial tensions, γ_{13}, between silica **1** and different solutions **3**, as there is a degree of uncertainty in determining the point of zero separation and, hence, the accuracy of C_1 in AFM force measurement. Note also that there are relatively little changes among the values of D_1 and C_2 given in Table 3.2. On the other hand, there are significant variations in the values of D_2 obtained in different solutions.

The different solutions of organic solutes used for the AFM force measurements may be divided into three groups, depending on their D_2 values. The first group consists of Nanopure water, 2% pyridine solution, and 10% TFE solution. The interactions between the glass sphere and silica plate exhibited hydration forces with their D_2 values in the range of 2.1-2.4 nm. The second group consists of 10 and 20% ethanol solutions, which give D_2 values in the range of 1.1-1.2 nm. The third group consists of 15% methanol solution, in which silica surface gives no evidence for hydration force, i.e., D_2=0 nm

The fact that the measured hydration force decreases in the presence of organic solutes suggests that it is not due to the asperities or roughness of the silica surface. A similar suggestion was made by Meagher (30), who observed that the hydration force between silica surfaces disappears in 0.01 M $CaCl_2$ solution at pH 10.3. If it is assumed that the hydration force is a result of steric repulsion between silicic hairs on the silica surfaces, it is possible to attribute the observed disappearance to the collapse of the hairs due to the charge neutralization (19,31) in the presence of Ca^{2+} ions. On the other hand, it is also possible that the amount of Ca^{2+} ions adsorbing on silica under the conditions employed by Meagher was so large that the effect of the silica substrate may be masked. The silica surfaces covered by large amounts of Ca^{2+} ions may not create as strongly hydrated surfaces as those without. This view may be supported by the fact that the standard free energy of hydration (ΔG^0_{hyd}) for Si^{4+} ions is –26,220 kJ/mole while that of Ca^{2+} ion is –2,932 kJ/mole. These values were calculated from the formula (32): $\Delta G^0_{hyd} = -136.9 z^2 / r$ kcal/mole, where z is the valance of the cation under consideration and r is its radius.

Since the solutes used in the force measurements conducted in the present work are non-ionic, it is difficult to suggest that the silica hairs collapse due to charge neutralization or double-layer compression. It is also difficult to believe that the polymer-like hairs collapse (or retract) due to the poor solvent property of water. Furthermore, there seems to be no correlation between the values of the dielectric constants (ε_3) of the different solutions used in the force measurements and the decay lengths of the measured hydration forces. One possible explanation may be that the methanol and ethanol dehydrate silica surfaces and subside swelling, which has been considered to be a cause for the extraneous repulsion observed with silica surfaces.

Perhaps the most likely explanation for the decrease in the extraneous repulsion observed in the present work may be that the water structure in the vicinity of silica surface changes significantly in the presence of the solutes that give lower D_2 values. It is possible that some the solutes specifically adsorb on the surface of silica and cause changes in the structure of the vicinal water. Kosmulski and Matijevic (26) showed that the iso-electric point (i.e.p.) of silica shifts from

pH 2.0 to 2.5 in the presence of 10% methanol and ethanol, indicating that the short-chain alcohols adsorb specifically on the surface. The shift in i.e.p. towards higher pH suggests that the number of positively-charged sites, which may be represented as $Si\text{-}OH_2^+$, increases in the presence of the alcohols. For this, the explanation given by Kosmulski and Matijevic was that alcohol molecules adsorb preferentially on the $Si\text{-}OH_2^+$ sites and stabilize them. The results of the force measurements obtained in the present work are consistent with this explanation. As shown in Figure 3.1, the force curves obtained in methanol and ethanol solutions can be fitted to the charge regulation model, while those obtained in Nanopure water can be fitted to the constant charge model. Thus, there is sufficient evidence that short-chain alcohols adsorb on silica from aqueous solutions. One of the mechanisms controlling the adsorption process would be the acid-base interaction, with silanol acting as acid and alcohol as base. Since the adsorption process occurs in solution, it is necessary that alcohol displace water molecules. It may be possible to determine whether the displacement reaction can occur or not by comparing the pK_b values for water and the alcohols which are given in Table 3.2.

Recall that the hydration force disappears completely at 15% methanol, and that the force curve can be fitted to the DLVO theory perfectly. The disappearance of the hydration force in 15% methanol solutions may be attributed to the changes in the hydration layer in the vicinity of silica, which in turn was caused by the adsorption of methanol. The fact that the pK_b (=15.2) of methanol is smaller than that (pK_b=15.7) of water supports this view. That the pK_b difference between the two is relatively small may explain the fact that a relatively high concentration of methanol is needed before the hydration force disappears completely. There are additional thermodynamic data indicating that water can be displaced by methanol, which is an essential part of the adsorption mechanism. Microcalorimetry studies (33) conducted on the adsorption of water and methanol from vapor phase showed that heats of adsorption are in the range of 25-45 kJ/mol for water and 55-65 kJ/mol for methanol. Clearly, methanol has a higher affinity than water for the silica surface.

The pK_b values of Table 3.2 show that ethanol is less basic than water. If the adsorption mechanism is controlled only by the acid-base interaction, ethanol should not adsorb on silica.

Jones and Mill (34) showed, however, that ethanol does adsorb on silica from solution. Therefore, there must be mechanism(s) other than the acid-base interactions controlling the adsorption process. One possibility may be that the hydrocarbon chains associate with each other, which should contribute to the increase in the negative adsorption free energy. It seems, nevertheless, that the driving force for the adsorption process is weak. According to Jones and Mill, its adsorbability is comparable to that of water, which is probably the reason that the hydration force does not disappear completely at high concentrations of ethanol.

At 2% pyridine, the hydration force does not change significantly from that observed in Nanopure water. The values of C_1, D_1, C_2, and D_2 for both are not too different from each other, as shown in Table 3.2 and Figure 3.3. This finding is unexpected in a sense that a basic molecule such as pyridine (pK_b=8.7) should adsorb on an acidic substrate such as silica and disrupt its hydration structure. Therefore, it would be of interest to determine whether pyridine adsorbs on silica or not. To answer this question, 5 g of BDH silica was contacted with a 10^{-4} M pyridine solution of pH 6.0 for 20 minutes, and the supernatant solution was subjected to UV analysis. The characteristic absorption bands decreased considerably, indicating that pyridine adsorbs on silica. In fact, Matzner, et al. (35) determined the standard free energy of adsorption (ΔG_{ads}^{o}) to be -14 kJ/mol (35). Since this value is smaller than the heat of adsorption of water vapor on silica, which is approximately 52 kJ/mole (36), these authors suggested that pyridine may adsorb on silica in such a way that the water molecules are not displaced from the first few adsorption layers. As suggested by Matzner et al., pyridine may adsorb via H-bonding. Thus, the pyridine adsorption may not severely disrupt the water structure in the vicinity of silica, which may provide an explanation for the observation that the hydration force remains unchanged in the 2% pyridine solution.

The force curve obtained at 10% TFE does not show an evidence for changes in hydration force. The values of C_1, D_1, C_2, and D_2 are close to those obtained in Nanopure water, as shown in Table 3.2. This finding suggests that TFE does not adsorb on silica, most probably due to its acidity. As has been noted, TFE should be more acidic than ethanol because of fluorine substituting hydrogen.

3.5 Conclusions

The results presented in this communication strongly suggest that the short-range repulsive forces observed with silica in Nanopure water is due to the hydration force. This may be attributed to the likelihood that silica is one of the most strongly hydrated solid judging from the small size and the formal charge of the Si^{4+} cation as explained earlier. In solutions containing methanol and ethanol, the silica surface may be dehydrated, resulting in a decrease in the hydration force. Another consequence of the dehydration is that the swelling of silica is reduced, which should also result in a decrease in the extraneous repulsion observed at short distances. In a recent communication by Ninham and Yaminsky (37), it was suggested that the non-DLVO forces, including hydration force, are due to the specific interactions involving ions at interfaces. They suggested further that the specificity can be accounted for by dispersion interactions. This explanation may be applicable to the secondary hydration forces observed at high electrolyte concentrations. In the present work, however, hydration forces are observed in the absence of electrolytes; therefore, the Ninham and Yaminsky's approach may not be applicable for the primary hydration forces observed with silica.

The discovery that short-chain alcohols reduce the hydration forces associated with silica may be extended to explaining the intoxication of humans by these substances. The alcohols may interact with lipid membranes and reduce the hydration forces, which may be the cause for the intoxication. Spectroscopic analysis of lipids membranes treated with alcohols show evidence for the displacement of bound water (38,39). According to the force data obtained in the present work, methanol should be more intoxicating than ethanol.

3.6 References

1. Derjaguin, B. V., and Landau, L. *USSR Acta Physicochim*. **14,** 633 (1941).
2. Verwey, E. J., and Overbeek, J. Th. G. *Theory of the Stability of Lyophobic Colloids* Elsiever, New York, 1947.
3. Israelachvili, J., and Pashley, R. M. *Nature* **300,** 341 (1982).
4. Rabinovich, Ya. I. and Derjaguin, B. V. *Colloids and Surfaces* **30,** 243 (1988).
5. Pashley, R. M., Mcguiggan, P. M., Ninham, B. W., and Evans, D. F. *Science* **229,** 1088 (1985).
6. Rabinovich, Ya. I., Derjaguin, B. V. and Churaev, N. V. *Adv. Colloid Interface Sci.* **16,** 63 (1982).
7. Peschel, G., Belouschek, P., Muller, M. M., Muller, R. M., and Konig, R. *Colloid Polymer Sci*. **260,** 444 (1982).
8. Horn, R. G., Smith, D. T., and Haller, W. *Chem. Phys. Lett.* **162,** 404 (1989).
9. Grabbe, A. and Horn, R. G. *J. Colloid Interface Sci*. **157,** 375 (1993).
10. Ducker, W. A., Senden, T. J., and Pashley. R. M. *Nature* **353,** 239 (1993).
11. LeNeveu, D. M., Rand, R. P., and Parsegian, V. A. *Nature* **259,** 601 (1976).
12. Derjaguin, B. V., and Churaev, N. V. *Colloids Surf.* **41,** 223 (1989).
13. Allen, L. H. and Matijevic, E. J. *Colloid and Interface Sci.* **31,** 287 (1969).
14. Watillon, A. and Gerard, PH. *Proc. Int. Congr. Surface Activ.* **4,** 1261 (1964).
15. Pashley, R. M. *J. Colloid Interface Sci*. **83,** 531 (1981).
16. Israelachvili, J. N., and Pashley, R. M. *Nature* **306,** 249 (1983).
17. Yotsumoto, H., and Yoon, R-H. *J. Colloid Interface Sci.* **157,** 434 (1993).
18. Ducker, W. and Pashley, R. M. *Langmuir* **8,** 109 (1991).
19. Israelachvili, J. N. *Intermolecular and Surface Forces*, 1st ed.; Academic Press, New York, 1991.
20. Vigil, G., Xu, Z., Steinberg, S., and Israelachvili, J. N. *J. Colloid Interface Sci.* **165,** 367 (1994).
21. Yaminsky, V. V., Ninham. B. W. and Pashley, R. M. to be published
22. Yotsumoto, H., Yoon, R-H, Wakamatsu, T, Ito, S., and Sakamoto, H. *J. Min. Mat. Pro.*

Ins. Japan **110,** 511 (1994).

23. Rabinovich, Ya. I. and Yoon, R.-H. *Colloids and Surfaces,* **93,** 263 (1994).
24. Senden, T. J. and Ducker, W. A. *Langmuir* **10,** 1003 (1994).
25. Chan, D. Y. C., Pashley, R. M., and White, L. R. *J. Colloid Interface Sci.* **77,** 283 (1980).
26. Kosmulski, M. and Matijevic, E. *Langmuir* **8,** 1060 (1992).
27. Hough, D. B. and White, L. R. *Adv. Colloid and Interface Sci.* **14,** 3 (1980).
28. McMurry, J. *Organic Chemistry*, 2nd ed.; Wadsworth, Inc., Belmont, California, 1988.
29. Gyenes, I. *Titration in non-aqueous media*, D. Van Nostrand Co., Inc. New Jersey, 1967.
30. Meagher, L. *J. Colloid Interface Sci*. **152,** 293 (1992).
31. Israelachvili, J., and Wennerstrom, H. *Nature* **379,** 219 (1996).
32. Harvey, K. B. and Porter, G. B. *Introduction to Physical Inorganic Chemistry,* Addison-Wesley Publishing Co., Inc., 1963.
33. Bolis. V, Cavengo. A., and Fubini. B. *Langmuir* **13,** 895 (1997).
34. Jones, D. C., and Mill, G. S. *J. Chem. Soc.* 213 (1957).
35. Matzner, R. A., Bales, R. C. and Pemberton, J. E. *Applied Spectroscopy* **48, no. 9,** 1043 (1994).
36. Kiselev, A. V. *Zh. Fiz. Khim*, **35,** 233 (1961).
37. Ninham, B. W., and Yaminsky, V. *Langmuir* **13,** 2097 (1997).
38. Chiou, J. S., Ma, S-M, Kamaya, H., and Ueda, I. *Science* **248,** 583 (1990).
39. Yurttas, L.; Dale, E. B.; and Klemm, W. R. *Alcoholism: Clin. Exp. Res.* **16,** 863 (1992).